Current Biology, Vol. 15, 2179–2189, December 20, 2005, ©2005 Elsevier Ltd All rights reserved. DOI 10.1016/j.cub.2005.11.037

Article

Cerebellar Complex Spike Firing Is Suitable to Induce as Well as to Stabilize Motor Learning

Nicolas Catz,[1] Peter W. Dicke,[1] and Peter Thier[1,*]
[1] Department of Cognitive Neurology
Center of Neurology
University of Tübingen
Hertie Institute for Clinical Brain Research
Ottfried Müller Strasse 27
72076 Tübingen
Germany

Summary

Background: Cerebellar Purkinje cells (PC) generate two responses: the simple spike (SS), with high firing rates (>100 Hz), and the complex spike (CS), characterized by conspicuously low discharge rates (1–2 Hz). Contemporary theories of cerebellar learning suggest that the CS discharge pattern encodes an error signal that drives changes in SS activity, ultimately related to motor behavior. This then predicts that CS will discharge in relation to the error and at random once the error has been nulled by the new behavior.
Results: We tested this hypothesis with saccadic adaptation in macaque monkeys as a model of cerebellar-dependent motor learning. During saccadic adaptation, error information unconsciously changes the endpoint of a saccade prompted by a visual target that shifts its final position during the saccade. We recorded CS from PC of the posterior vermis before, during, and after saccadic adaptation. In clear contradiction to the "error signal" concept, we found that CS occurred at random before adaptation onset, i.e., when the error was maximal, and built up to a specific saccade-related discharge profile during the course of adaptation. This profile became most pronounced at the end of adaptation, i.e., when the error had been nulled.
Conclusions: We suggest that CS firing may underlie the stabilization of a learned motor behavior, rather than serving as an electrophysiological correlate of an error.

Introduction

Visual targets are fovealized by converting a retinal vector, defining the location of the target on the retina relative to the fovea into a command for a saccade that moves the target image onto the fovea. The transformation of the retinal vector into the saccade vector is under adaptive control in humans as well as in monkeys as, for instance, demonstrated by the time-dependent consequences of eye muscle palsy [1]. If an extraocular muscle is weakened, the saccades involving this muscle will typically be of lower velocity and too-small amplitude, because the saccade command is executed by an insufficient effector. However, provided the palsy is not too severe, after a few days the saccade amplitude may become normal again, reflecting the fact that one and the same retinal vector is translated into a changed motor command, able to override the insufficiencies of the peripheral effector. The flexibility of the relationship between the retinal vector and the saccade command can be demonstrated by resorting to a simple paradigm, often referred to as short-term saccadic adaptation, first described by McLaughlin [2] (see Hopp and Fuchs [3] for review). In this paradigm (see Figure 1 for an illustration), the subject has to make a saccade toward a peripheral visual target. Then, while the eyes move toward the target, the target is shifted to a nearby position. Due to the suppression of vision during saccades, the subject is unaware that the target is moved and the eyes arrive at where they expected the target to be. Since the target is missed by the primary saccade, a corrective saccade has to be added. However, if these target shifts are repeated time and again in a consistent manner, one typically observes that the metrics of the primary saccade change, such as to bring the eyes closer to the final location of the target. In other words, a given retinal vector is remapped onto a new saccade vector. This remapping is a form of motor learning that critically depends on the integrity of a specific part of the cerebellum known to contain a representation of saccadic eye movements, namely the posterior vermis, comprising lobules VI and VII. This is indicated by the fact that experimental lesions of the posterior vermis cause an irreversible loss of short-term saccadic adaptation, while the initial saccadic dysmetria subsides over time [4]. What is the neuronal basis of short-term saccadic plasticity in the posterior vermis? An answer to this question may lead to a better understanding of cerebellar learning at large. Cerebellar cortex depends on two inputs: the mossy fiber afferents, serving parallel fiber input to cerebellar Purkinje cells (PC), and the climbing fiber afferents, directly contacting the PC. An influential theory of learning [5, 6] (the Marr-Albus theory), originallly suggested by David Marr, tries to lead learning back to a specific interaction between signals conveyed by these two cerebellar afferent systems. Learning is thought to be a direct consequence of changing the strength of the synapses from parallel fibers onto PCs, a change in synaptic efficacy that is translated into changes of the SS discharge of P cells, dominating the cerebellocortical outflow. The second afferent system, the climbing fiber system, is thought to be the cause of these changes. Specifically, this theory assumes that climbing fiber activity responsible for the CS fired by P cells serves as the "teacher," conveying information on the size and/or direction of the motor error, needed in order to change the weights of the parallel fibers synapses in an appropriate manner [5, 6]. If this concept is correct, CS spike trains should convey information on the size and/or direction of the motor error during saccadic adaptation. In this case, we would expect CS spike trains to exhibit specific

*Correspondence: thier@uni-tuebingen.de

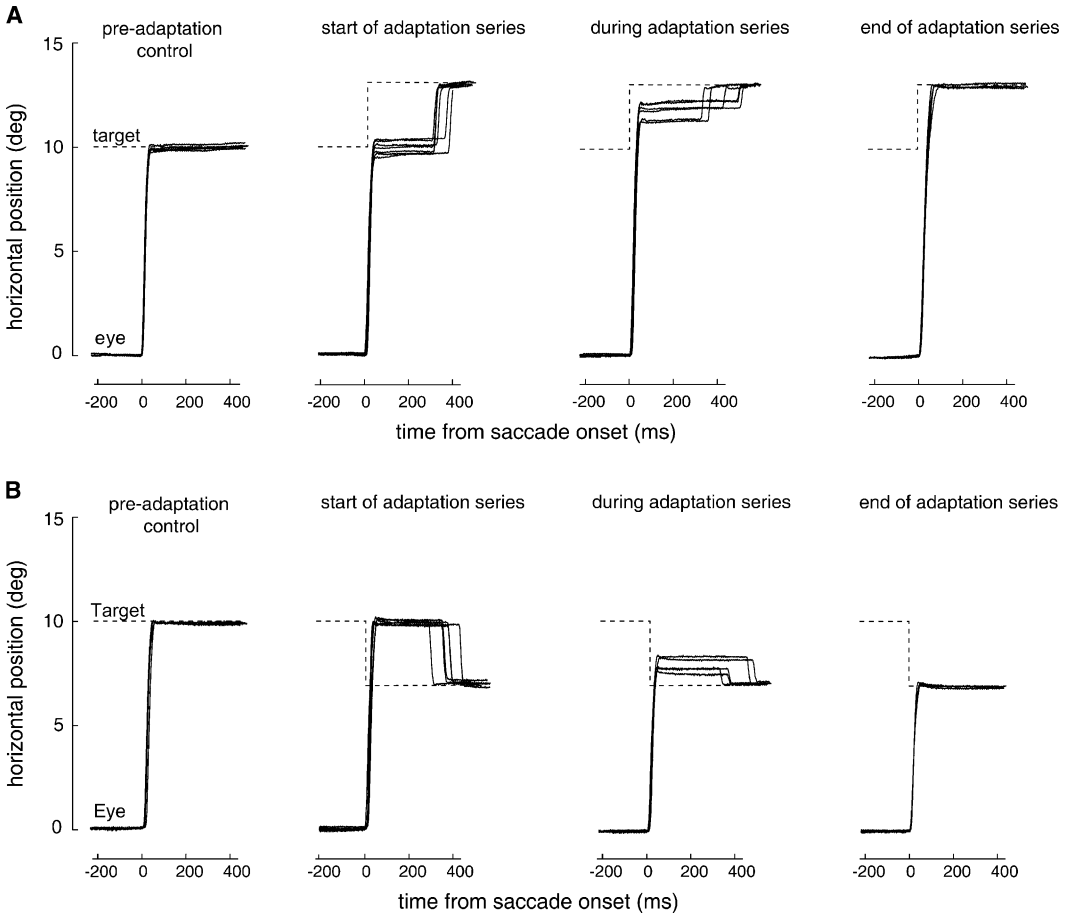

Figure 1. Examples of Trials Illustrating Saccadic Adaptation

Examples of eye movement records demonstrating the progress of outward (A) and inward (B) adaptation of horizontal visually guided saccades. The target jumped 10° to right. It either stayed there (preadaptation control) or moved to a new location during the saccade, either further out to 13° (outward adaptation) or back in the direction of the fixation point to an eccentricity of 7° (inward adaptation). Each panel shows the horizontal eye and horizontal target position. The records shown in the third panels were obtained after about 700 trials, those representing the end state of saccadic adaptation after 1000 trials.

saccade-related profiles early during saccadic adaptation, when the motor error is maximal. Conversely, CS should discharge at random once the error has been nulled and the new optimal saccade metrics have been established. In order to test these predictions, we analyzed the CS responses of vermal PCs of rhesus monkeys recorded before, during, and after saccadic adaptation as induced by a standard short-term saccadic adaptation paradigm. The results obtained are in clear contradiction to the predictions of the "error signal" concept. We found that CS occurred at random before adaptation onset, i.e., when the error was maximal, and built up to a specific saccade-related discharge profile only during the course of adaptation. This profile became most pronounced at the end of adaptation, i.e., when the error had been nulled, and actually outlasted the end of the adaptation process.

Results

In the example characterized in Figure 1, a peripheral visual target appears at 10° to the right of the central fixation spot, signaling the monkey to move his gaze away from the fixation spot toward this target. In contrast to trials of undisturbed visually guided saccades (Figures 1A and 1B: preadaptation control), during adaptation trials, the target is displaced either a few degrees further out ("outward adaptation," target shift by 3° in Figure 1A: start of adaptation series) or alternatively a few degrees back toward the fixation point (Figure 1B: start of adaptation series). During the first trials of adaptation, the monkey's eyes typically land at the location where the target had been before the shift, requiring a second, corrective saccade to reach the final location of the target. However, after several hundred consistent repetitions of such intrasaccadic target displacements (i.e., on alternative blocks either out or in), the amplitude of the first saccade increases (outward adaptation, Figure 1A) and decreases (inward adaptation, Figure 1B) gradually until, at the end of adaptation in the examples described in Figure 1, a 10° target may elicit 13° (outward adaptation) and 7° (inward adaptation) saccades. In other words, as a consequence of adaptation, a given retinal vector is mapped onto a new motor vector.

Extracellular recordings of CS of 382 Purkinje cells (PC) in vermal lobules VI and VIIA of two rhesus monkeys

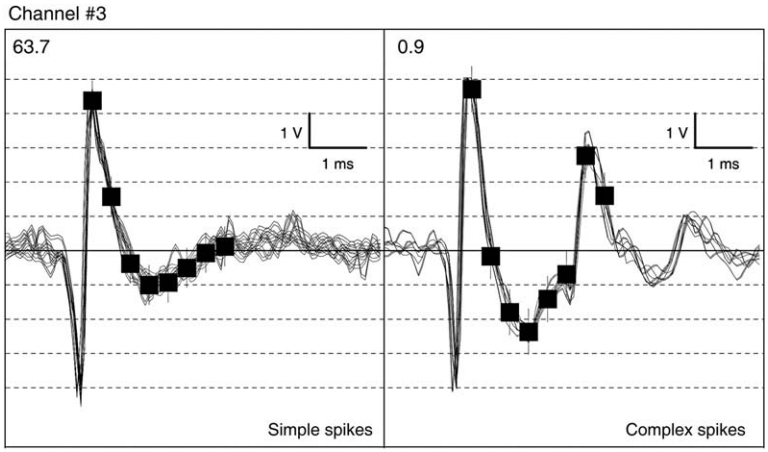

Figure 2. Example of Simple and Complex Spikes Recorded from a Single Purkinje Cell, Separated by a Multispike Detector Described in the Text

The squares define the 8-point template against which the records are compared. Note the consistency of the individual waveforms, detected as simple and complex spike waveforms. The temporal extent of each window is 6.6 ms. Note that the volt scale refers to an amplified signal.

(272 in monkey N and 110 in monkey E) were taken while the monkeys performed visually guided saccades before (preadaptation trials), during, and after saccadic adaptation. Individual PC were randomly assigned to inward or outward adaptation tasks. Of the 382 PC, 172 stable recordings were taken during the full course of adaptation including a preadaptation period (see Experimental Procedures and Figure 2 for example of record showing the two types of spikes fired by PC). Of these 172 PC, 98 were studied during outward adaptation and 74 during inward adaptation. Figure 3 depicts representative raster plots of CS responses (left) with plots of mean saccade amplitude (right) before, during, and after outward (Figures 3A and 3B) and inward (Figures 3C and 3D) adaptation. The CS events of the preadaptation trials are represented below the horizontal dashed line and subsequent adaptation trials are plotted in increasing order above the line. The vertical dashed line indicates the end of the primary saccade (saccade offset). None of the four exemplary neurons illustrated exhibited saccade-related CS responses during the preadaptation period. Saccade-related CS responses developed only after adaptation onset and reached their final form only after stable adaptation had been achieved. The shape of the response depended on the direction of adaptation. As exemplified for outward adaptation (Figures 3A and 3B), the CS discharge developed a perisaccadic pause whose duration increased in parallel with the increase in saccade amplitude. Of 98 PC tested, 73 (74.5%) displayed this pattern. Only a minority of the 98 neurons (n = 17, 17.3%) showed a slight increase in CS discharge around the saccadic eye movement (at the time of the perisaccadic pause described previously) or, alternatively (n = 8, 8.2%), lacked the development of any noticeable saccade-related change in CS firing. The timing of the perisaccadic pause emerging during adaptation varied between neurons. For instance, in the case of the PC in Figure 3A, the pause started 150 ms before and ended 70 ms after saccade offset. On the other hand, the pause exhibited by the second PC shown (Figure 3B) ended later, at about 100 ms after saccade offset, and also started conspicuously later. In both examples, the target initially appeared at an eccentricity of 10° and then jumped further outward to 13° during the saccade. As shown in the panels to the right of the raster plots, illustrating the means and standard errors of the primary saccades, saccade amplitude gradually increased in the course of outward adaptation until approaching 12° after 400–500 trials (t test comparison of mean pre- and postadaptation amplitudes, $p < 0.01$). As can be seen, the perisaccadic pauses became maximal only when the maximal changes in saccade amplitude were observed. During inward adaptation from 10° to 7.5° (t test comparison of mean pre- and postadaptation amplitudes, $p < 0.01$), the probability of observing a CS during and shortly after the saccade increased in the overwhelming majority of PC (52/74, 70.2%; see Figure 3C for an example). Only a minority of neurons (n = 13, 17.5%) exhibited a decrease comparable to that seen during outward learning. For nine neurons, no change was observed. In the example shown in Figure 3C, a perisaccadic synchronization of CS around saccade offset gave rise to a "burst," followed by a dip. The PC exemplified in the raster plot in Figure 3D showed a qualitatively similar, albeit less conspicuous, pattern. Moreover, the "burst-dip" sequence emerged much later during adaptation. In summary, inward and outward adaptation give rise to qualitatively different CS response patterns in the majority of PC, although quantitative differences in the strength and the timing of these patterns among individual PC are noted. How important are the quantitative differences in CS patterns of individual PC?

Several hundred PC converge on individual deep cerebellar nuclei neurons [7]. Therefore, it seems likely that at the level of the caudal fastigial nucleus (cFN), the part of the cerebellar nuclei targeted by posterior vermal PC axons, the discharge patterns of individual PC are no longer discerned, and it is the collective discharge of larger groups of PC that matters. Moreover, the discharges of these next-stage neurons are most probably dominated by the much more numerous PC SS, rather than by the CS, which are poorly transmitted down the Purkinje cell axon [8]. Hence, although individual CS may have the potential to change individual SS patterns, these individual differences will tend to be averaged out at the level of the cFN. With these considerations in mind, we calculated CS population responses based on the two samples of PC studied during outward and inward adaptation, respectively, in order to capture the overall effect on saccadic adaptation. Figure 4 shows these CS population responses for outward (Figure 4A)

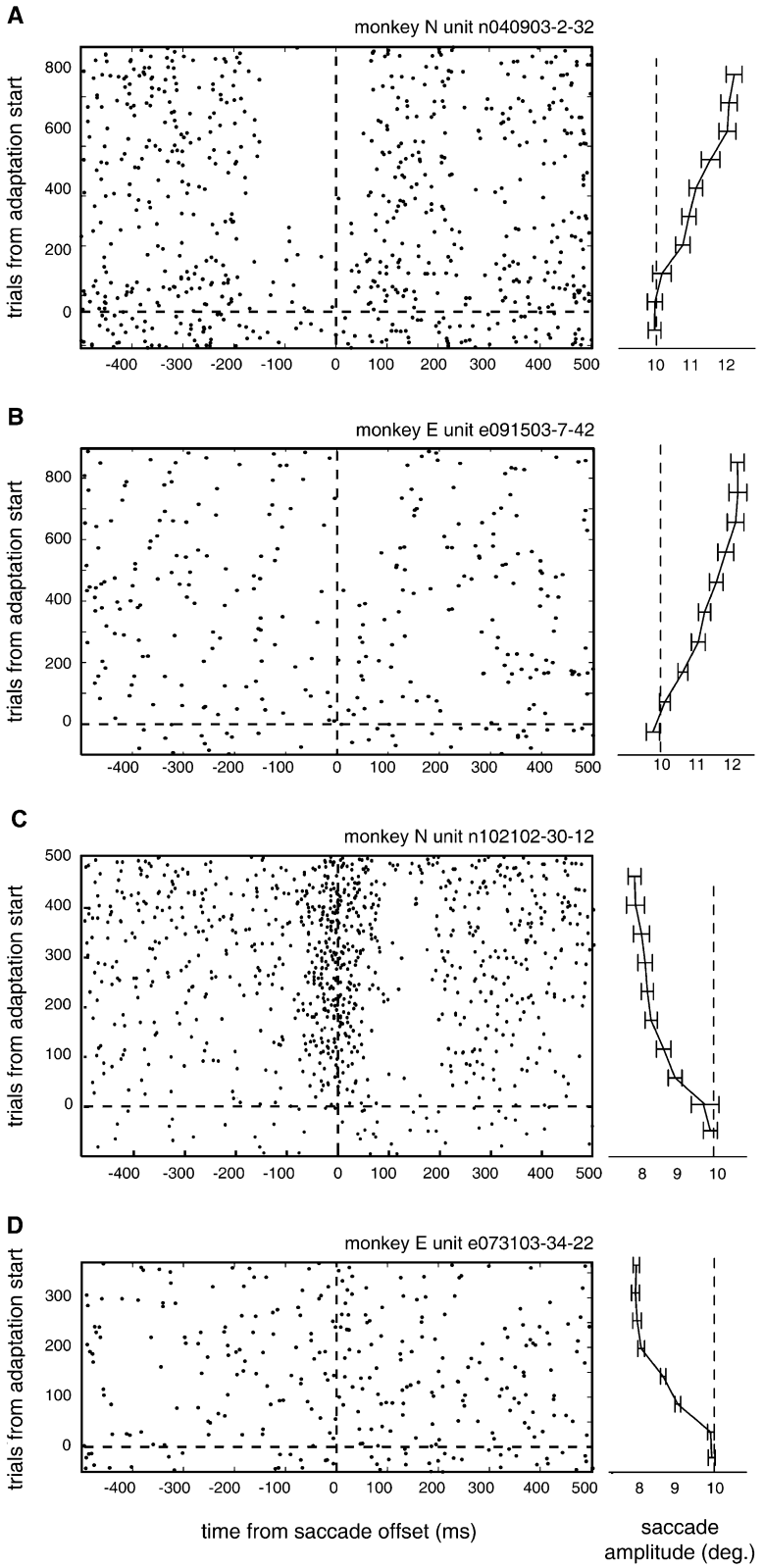

Figure 3. Examples of CS Discharges during Saccadic Adaptation

Raster plots illustrating the CS discharge of representative PC before, during, and after outward (A and B) and inward (C and D) saccadic adaptation. The x axis plots time relative to saccade offset at 0 marked by vertical lines. Lined up along the y axis are individual trials of saccades, the bottom ones up to the horizontal line without intrasaccadic target displacements (target position: 10º) and the following ones reflecting the progress from no adaptation (bottom) to full adaptation (top), with displacement of the target to 12.5º (A and B) and 7.5º (C and D). Each dot marks the occurrence of an individual CS. Right of the each raster panel, mean (±SEM) amplitude of the primary saccade before and during adaptation.

and inward (Figure 4B) adaptation as they developed over time relative to saccade offset (t = 0) on the x axis and for different states of adaptation plotted along the y axis. Since stable adaptation was reached after varying numbers of trials, we described the time course of adaptation by dividing the overall period of time until stable adaptation into 20 equally spaced time bins independent of the absolute number of trials involved. The color code represents the mean CS rate for a particular point in time and state of adaptation. There was no

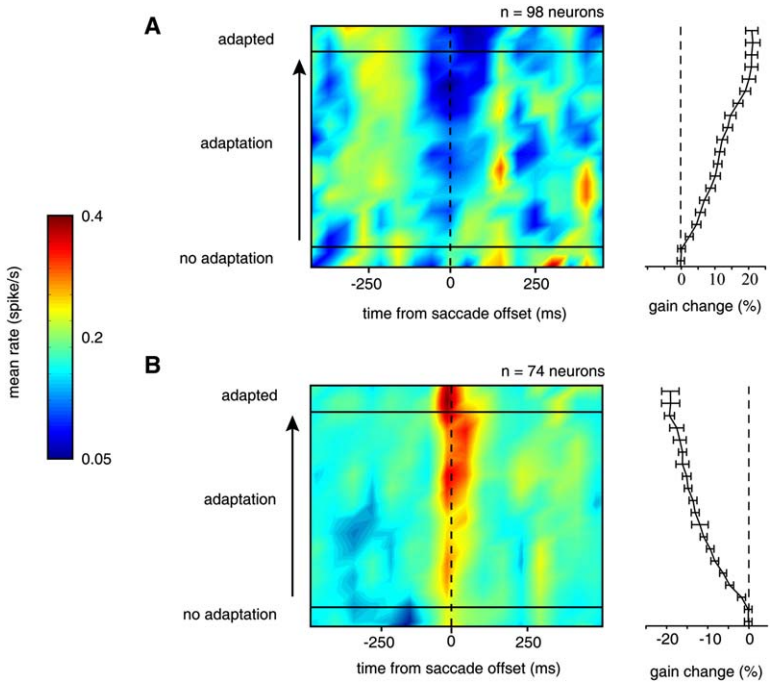

Figure 4. Change in Complex Spike Population Responses in the Course of Adaptation

(A) The left panel depicts the population response based on 98 posterior vermal PC studied during outward adaptation, and the right panel shows the mean saccadic gain change (±SEM) as a function of adaptation level for the 54 outward adaptation sessions that were necessary to collect the PC contributing to the population data.

(B) The left panel shows the population response for 74 posterior vermal PC (not overlapping with the "outward" population) studied during inward adaptation. The right panel depicts saccade gain change (±standard error) as a function of adaptation level based on 42 inward adaptation sessions that were required to collect the sample of PC. Complex spike population responses are plotted as function of time relative to saccade offset (x axis) and normalized adaptation level (y axis) from no adaptation (horizontal line) to full adaptation (top). The part underneath the horizontal line represents trials prior to the onset of target displacements. The color code represents the mean rate of CS activity in the population for time bins of 25 ms (x axis) and adaptation bins, corresponding to 1/20 of the range from no to full adaptation. We used a Gaussian filter (SD 50 ms) to smooth the plot along the x axis.

noticeable saccade-related CS modulation of the population before the onset of either inward or outward adaptation. However, during learning, the CS population responses changed. During outward adaptation, the CS population gradually developed a profound perisaccadic pause around saccade offset. The perisaccadic pause was maximal and, moreover, stable when the new saccade amplitude had been achieved (learned), and the new saccade amplitude stabilized as shown in the panel on the right of the population response plot (Figure 4A), depicting the mean population gain change for the 54 outward adaptation sessions needed to record the 98 neurons contributing to the population response. In contrast to outward adaptation, the population response for inward adaptation was characterized by the emergence of a conspicuous increase in the CS response around saccade offset (Figure 4B). This increase was largest at the end of learning, when the saccadic gain was stably decreased (Figure 4B), suggesting that the CS can hardly encode the size of the motor error. Nevertheless, in order to assess the relationship of CS firing and the size or direction of the motor error more rigorously and to exclude the possibility that the CS response reflects characteristics of the motor error, we decided to quantify the information conveyed by CS on the size and direction of the motor error by resorting to a sensitive statistical analysis of information content introduced by Kitazawa and coworkers [9] into the analysis of complex spike-firing patterns. This analysis builds on the assumption that the probability of observing CS should be higher in trials with large motor errors than in trials with small motor errors, if CS provide information on the size of the motor error. Conversely, CS will be distributed evenly in trials with large and small motor errors if they occurred independent of the size of the motor error. In order to test whether the distribution of CS reflected the size of the motor error, we assigned all trials of an adaptation run to one of two pools, where the first one contained the 50% of trials with the smallest motor errors and the second one contained the 50% of trials with the largest motor errors. Obviously, if both classes contain equal numbers of CS, the CS does not predict the size of the motor error. Correspondingly, the "information transmission rate" (I_r) variable, basically a measure of the asymmetry of the distribution between the two pools (see Experimental Procedures for its exact definition), would be zero. Conversely, if all CS observed fell into only one of the two classes, the CS would be a perfect predictor of the motor errors represented by that particular class and the I_r would become maximal.

Figure 5 exemplifies the results of the information content analysis for a neuron tested during an outward adaptation. Figures 5A and 5B depict the evolution of the motor error and the amplitude of the primary saccade, respectively, during the course of adaptation. Before adaptation the motor error is close to zero; it is maximal at learning onset; and it decreases gradually during adaptation and is close to zero after adaptation. If the CS response reflected either the direction or the size of the error, the maximal CS response modulation should be observed when the error is maximal.

Figures 5C and 5D illustrates the probability of the occurrence of CS within a period of 200 ms after saccade onset, thought to be critical for the assessment of the efficacy of a primary saccade and the extraction of the resulting motor error. The blue dots in Figures 5C and 5D depict the trials in which no complex spike was observed in the given time window. In contrast, the red dots represent the trial in which a complex spike was

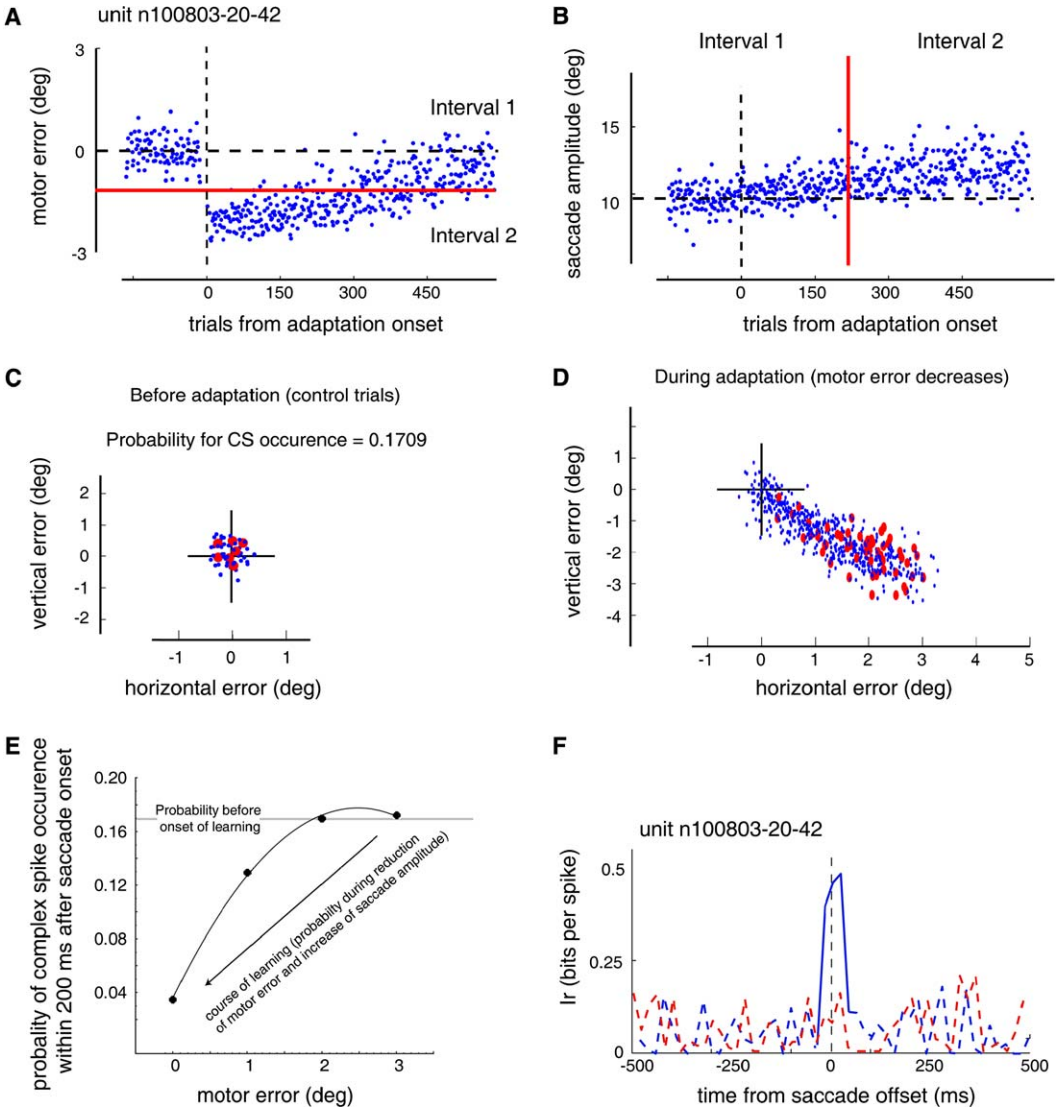

Figure 5. Example of Purkinje Cell Tested during Outward Adaptation

(A) Evolution of the motor error during learning as function of trial number from adaptation onset. The red line depicts the median of motor error used in order to separate the two pools.

(B) Evolution of saccade amplitude during learning.

(C and D) Scatterplots of the error in the trials without complex spike during the first 200 ms after saccade onset (blue dots) and in the trials with complex spikes (red dots).

(C) Scatterplots of the trials collected before adaptation onset: control trials.

(D) Scatterplot of the motor errors collected during outward adaptation.

(E) Probability (p) of complex spike occurrence during the first 200 ms after saccade onset as a function of the motor error. Before learning (motor error = 0), p = 0.1709 (less than one complex spike detected for five trials); at adaptation onset (motor error maximal), p = 0.1724; after full and stable adaptation, p = 0.0348.

(F) Information transmission rate (I_r) for motor error (red curve) and saccade amplitude (blue curve). I_r encoded by the complex spikes of the Purkinje cell described previously. I_r plotted as a function of the time relative to saccade offset. Solid and broken traces depict significant and non-significant information, respectively.

recorded. Figure 5C presents the trials collected before adaptation onset (control trials), whereas Figure 5D depicts the trials collected during a full run of outward adaptation, in which an initial error of 3° was completely nulled at the end. The fact that the blue dots and the red dots are spatially congruent in both figures clearly speaks against a representation of the motor error in the CS discharge in the time window considered. On the other hand, as shown in Figure 5E for the same neuron, the probability of seeing CS within the window of 200 ms after saccade onset changed gradually and consistently during saccadic adaptation. It was 0.1709 before adaptation onset, at a time when the motor error was zero. Early during adaptation, when motor error was large, the probability was not different from the preadaptation value (p = 0.1724). During learning, the probability decreased and reached a minimal value when the error was close to zero (p = 0.0348), now being clearly

different from the one observed before learning when the error was zero. A look at the information transmission rate I_r for this neuron given in Figure 5F demonstrates that the lack of a reflection of the motor error is not specific to the period of 200 ms after saccade onset considered in Figures 5C–5E. This figure shows I_r as function of time relative to saccade offset calculated for both the motor error (red curve) as well as for saccade amplitude (blue curve). Whereas I_r was not significantly different from zero for the motor error, the information on the absolute saccade amplitude (highly correlated with trial number) was significant for a period of about 100 ms aligned with the saccade offset (blue curve).

This result pertains to the whole population of PC CS studied. As shown in Figure 6 for outward (Figure 6A) and for inward (Figure 6B) adaptation, I_r, the measure of the information on motor error conveyed by CS, remained not significantly different from zero (dashed red curve), independent of time relative to saccade offset and independent of the direction of adaptation. On the other hand, CS provide information on the state of learning, as indicated by the fact that I_r, the information provided by CS on saccade amplitude (or trial number; blue curve), was significantly elevated for a period of about 200 ms, starting slightly before saccade offset. In other words, the statistical analysis clearly supports the first sight impression conveyed by the population averages, namely that CS patterns build up as function of time or adaptation state during adaptation rather than reflecting the motor error.

In order to determine more precisely the timing of the changes of firing in the population of CS, we next calculated an index comparing the saccade-related CS modulation as a function of time relative to saccade offset for time bins of 50 ms (20 bins). This CS modulation index CSM_i for a given bin i was defined as the contrast measurement of the baseline CS population discharge in a reference bin during stable fixation (−500 to −400 ms relative to saccade offset: $Activity_{ref}$) relative to the population discharge in bin i $Activity_i$:

$$CSM_i = \frac{Activity_{ref} - Activity_i}{Activity_{ref} + Activity_i}.$$

In order to capture the influence of adaptation on CS modulation, we compared CSM_i before and after stable adaptation by calculating the difference $D_i = CSM_{i\text{-}nonadapted} - CSM_{i\text{-}adapted}$.

Figure 7A plots D_i for inward (thick line) and outward (dashed line) adaptation as a function of time relative to saccade offset and fitted by Gaussians, which are relative mirror images as both diverge noticeably from 0 around −100 ms and peak around saccade offset. The only major difference between the two Gaussians is the sign being positive for inward and negative for outward adaptation. To assess the variability in the contributions of individual PC, we calculated the individual mean CS modulation CSM for all neurons included in the population responses in the period of time corresponding to the means ± standard deviations of the Gaussians (for inward, the Gaussian peaks at −23 ms, halfwidth 135 ms; maximal modulation between [−23 − (135/2)] = −90 ms and [−23 + (135/2)] = 45 ms after saccade offset; for

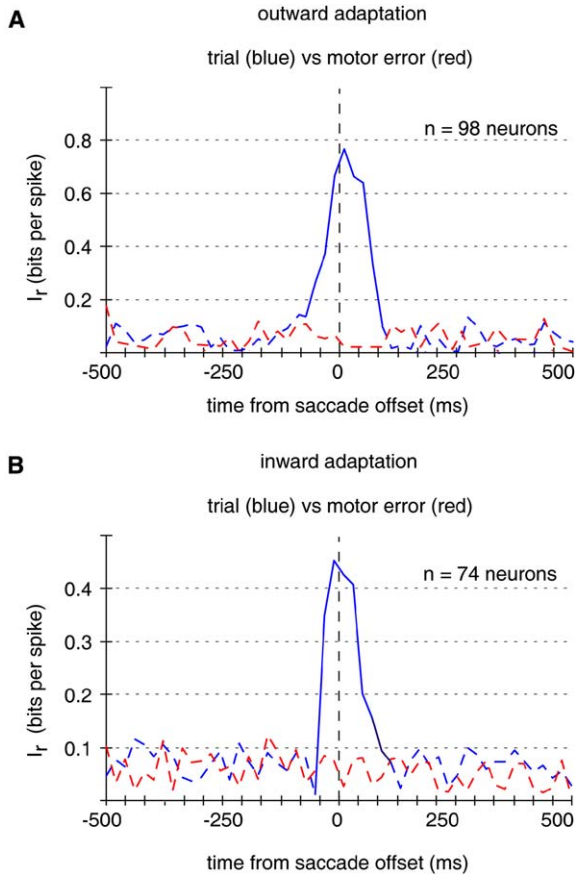

Figure 6. Population Information Transmission Rate

(A and B) Plots of mean I_r (information transmission rate), the measure of information provided by CS on the motor error (red) and the evolution of saccade amplitude (blue), respectively. See Experimental Procedures for equation used. Solid and broken traces depict significant and nonsignificant information, respectively.

outward, the Gaussian peaks at −10 ms, halfwidth 180 ms: maximal modulation between −100 ms and 80 ms). Figure 7B plots CSM for each PC after learning ($CSM_{adapted}$) as a function of the CSM before learning ($CSM_{nonadapted}$). The open circles represent neurons recorded during outward adaptation, and the filled circles represent those studied during inward adaptation. The ellipses fitted to the data delineate the confidence intervals (95%) for the two populations. When $CSM_{nonadapted} < CSM_{adapted}$ (dots located above the reference line; slope = 1), the CS activity of the neuron decreased in the given time window. By contrast, when $CSM_{adapted} < CSM_{nonadapted}$, the CS discharge increased. Irrespective of some overlap, the two ellipses for outward and inward adaptation differ significantly and lie on opposite sides of the bisector (t test, $p < 0.001$), indicating no change. The qualitative difference in the effects of outward and inward adaptation can similarly be retrieved, if one compares the population means and standard errors of the individual CSM_i before and after learning (Figure 7C). The mean $CSM_{nonadapted}$ (white columns) for outward and inward adaptation are not significantly different from 0 ($CSM_{nonadapted}$ inward 0.02632 ± 0.2157; $CSM_{nonadapted}$ outward 0.009 ± 0.201805; t test, $p > 0.05$) and not significantly different from each other

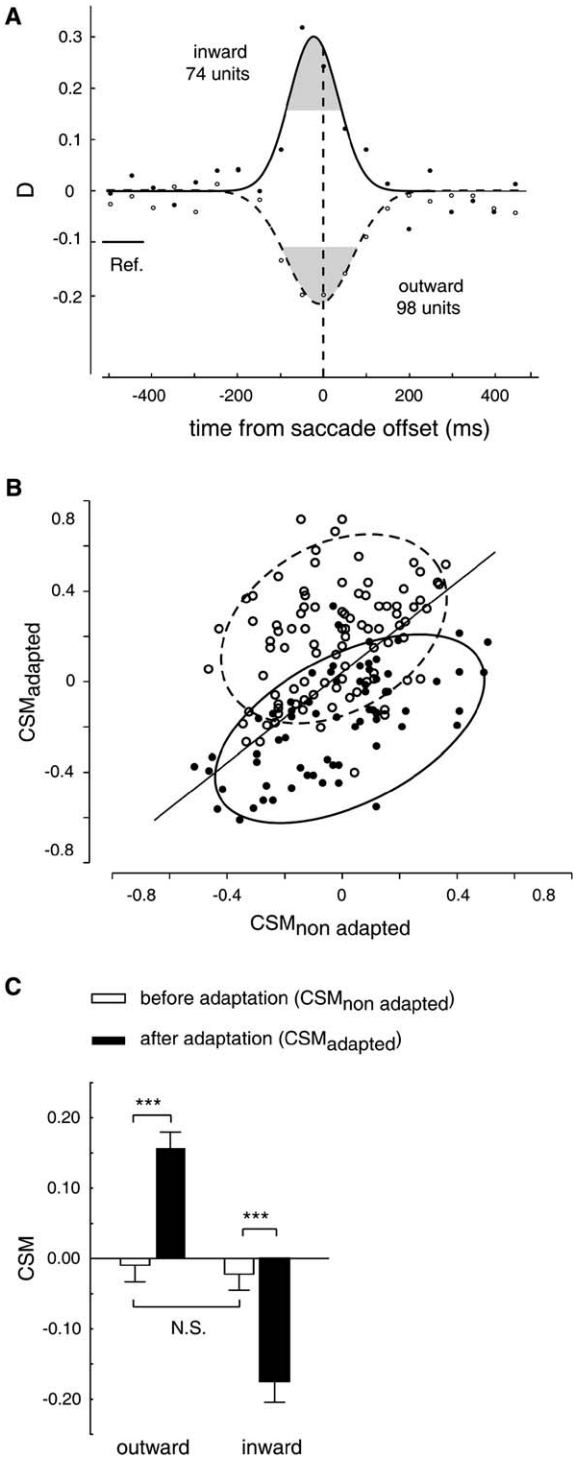

Figure 7. Quantitative Analysis of CS Discharge Modulation

Modulation of CS population discharge (A) captured by the modulation index D (see text for explanation) after adaptation; filled circles, inward adaptation; open circles, outward adaptation. The curves fitted to the individual data points are Gaussian functions [f(x) = a *exp $(-((x - b)/c)^2)$] with a = 0.2967, b = −23 ms, c = 81 ms, R^2 = 0.62 (half-width = 135 ms) in the case of inward learning, and a = −0.2185, b = −10 ms, c = 108 ms, R^2 = 0.73 (half-width = 180 ms) in the case of outward learning.

(B) Plot of CS modulation of individual PC as expressed by the coefficient CSM after full adaptation (see text for explanation) as function of CSM at the onset of adaptation for the time windows shown in gray in (A). The filled circles represent PC tested during inward adaptation, and the open circles indicate those recorded during outward adaptation. The ellipses describe the confidence interval (95%) of the data points for inward and outward adaptation, respectively. The diagonal line gives the location of PC, not showing changes of their CSM from no adaptation to full adaptation.

(C) Mean CSM before ($CSM_{nonadapted}$) and after ($CSM_{adapted}$) saccadic adaptation. Vertical bars, standard error. ***p < 0.001; N.S., p > 0.05.

(t test, p > 0.05). However, after adaptation, the mean $CSM_{adapted}$ differ significantly from the prelearning $CSM_{nonadapted}$, the one for inward adaptation being negative ($CSM_{adapted}$: −0.174460 ± 0.2416; paired t test, p < 0.001), and the one for outward adaptation being positive ($CSM_{adapted}$: 0.157360 ± 0.235; paired t test, p < 0.001).

Discussion

Does the cerebellar CS encode a motor error as proposed by the Marr-Albus theory of cerebellar cortex [5, 6]? Our findings suggest that this is not the case, at least not for saccadic learning. According to the Marr-Albus theory, CS discharge modulations observed during saccadic adaptation should be maximal at learning onset and decline in parallel as the motor error decreases during the course of learning. On the contrary, we observed a gradual build-up of CS modulation during the course of motor learning, as confirmed by the information transmission rate analysis described. This gradual build-up was actually mirror symmetric for outward and inward adaptation. Moreover, it was fully maintained after completion of learning, i.e., at a time the motor error had been nulled, suggesting that the CS responses might actually be involved in stabilizing the modified saccade metrics. Our findings are consistent with preliminary observations of Kahlon and Lisberger [10] on a small group of 12 floccular P cells, studied during smooth pursuit eye movement adaptation. These authors reported that the CS responses of these cells seemed to become more prominent in the course of adaptation. The idea that specific CS responses, developing in the course of learning, may actually be needed in order to stabilize the learned behavior might provide a simple explanation of the fact that a disturbance of the climbing fiber input seems to reset the learned behavior as noted by Yakushin et al. [11]. These authors adapted the vestibuloocular reflex (VOR) of monkeys by introducing appropriate visuo-vestibular conflicts. After the VOR gain had been decreased, they inactivated the nucleus of the optic tract (NOT), a major input to the inferior olive. The consequence of the NOT deactivation, which may be assumed to have indirectly hampered the climbing fiber signal relevant for VOR adaptation, was a return of the VOR gain toward the baseline value. A similar conclusion applies to a second VOR adaptation study, carried out by Demer and Robinson [12]. After increases or decreases of the VOR gain in the cat, inactivation of the inferior olive caused a rapid increase of the VOR gain. Conversely, electrical microstimulation of the inferior peduncle, routing the climbing fibers to the cerebellum, possibly mimicking the development of a specific CS pattern, caused an immediate decrease of the gain despite the absence of a visuo-vestibular conflict.

If the complex spike activity does not serve as a "teacher," reducing the motor error as suggested by the Marr-Albus theory, then the inferior olive cannot contain a representation of the motor error. Rather, as already suggested by Ito [13], the inferior olive seems to be downstream of a "comparator," extracting the instantaneous motor error during an ongoing movement by comparing the desired displacement and the actual displacement. With respect to saccades, the candidate structure serving as such a comparator might be the superior colliculus (SC). This is suggested both by its anatomical position relative to the inferior olive and its functional position in models of saccade generation. On the one hand, the SC projects heavily to the saccade-related parts of the inferior olive, the medial accessory olive (MAO) [14]. On the other hand, the SC is known to contain various types of neurons implicated in the control of saccades, among others the so-called build-up neurons that have been suggested to encode the instantaneous motor error [15–18]. While our findings are incompatible with a representation of the motor error at the level of the inferior olive, this does not imply that the CS discharge is necessarily independent of error information. For instance, the gradual build-up and later maintenance of the saccade-related CS responses observed would, in principle, be compatible with integration of error information derived from the SC by the inferior olive. The mechanism that could underlie this integration of the motor error in the inferior olive remains unknown. However, it seems close at hand to speculate that the feedback projection from the deep cerebellar nuclei, probably controlling the properties of intraolivary connectivity via GAP junctions [19] and thereby the amount of synchronicity of olivary neurons [20], may play a role.

Finally, we think that the reciprocal changes of the CS responses during inward and outward adaptation may provide the key to understanding the specific role of the CS in saccadic learning. Maximal long-term depression [21] at parallel fiber synapses is observed when a CS occurs within 200 ms after simple spikes [22]. Hence, the CS burst during inward adaptation peaking at −23 ms might induce LTD if the saccade-related SS burst appeared between −220 and −20 ms relative to saccade offset. Conversely, the suppression of CS during outward adaptation, maximal at −10 ms, might reduce LTD if the SS burst emerged between −210 and −10 ms. In other words, relative to nonadapted saccades, we would expect to see longer-lasting saccade-related SS activity in the case of outward adaptation but shorter-lasting saccade-related SS activity for inward adaptation. We have previously reported that the end of the Purkinje cell simple spike population burst (PB) gives a precise signature of the end of the saccadic eye movement [23]. Hence, if the PB end determined saccade offset, delaying the PB end would delay saccade offset and thereby increase the amplitude of the saccade. Conversely, reducing the duration of the PB would stop the saccade earlier and thereby lead to smaller amplitude saccades.

Conclusion

CS exhibit characteristic changes of their firing patterns during saccadic learning that are incompatible with a role of a teacher conveying feedback on a motor error. On the other hand, these changes would be optimally suited to maintain and stabilize the newly acquired behavior. There can be hardly any doubt that it is the SS that transports the learned behavior. Considering the well-established interaction of CS and SS firing provided by LTD, we suggest that cerebellar learning may be a consequence of CS sculpting specific patterns of SS activity underlying specific motor behaviors.

Experimental Procedures

Two monkeys (*Maccaca mulatta*) were prepared for chronic extracellular single unit and eye position recordings with search coils as described previously [24]. All animal procedures followed the guidelines set by the NIH and national law and were approved by the local committee supervising the handling of experimental animals.

Behavioral Procedures

The monkeys were asked to fixate a fixation spot located in the center of the monitor for periods of time that varied randomly between 1000 and 1500 ms. At the same time as the fixation spot went off, a target appeared randomly in one out of eight possible locations in the periphery at 0º, 45º, etc., having a constant distance from the center, varying between 2.5º and 20º in separate blocks. The monkeys were trained to execute prompt and very accurate saccades toward the peripheral target. After having determined the preferences of saccade-related PC (if such a Purkinje cell was isolated) in terms of saccade direction and amplitude, an adaptation series was started, using the standard "McLaughin" paradigm [2] in which the peripheral target moves in a predefined manner, while the saccade is carried out. When a saccade-related Purkinje cell was isolated, the direction of the adaptation corresponded to the preferred direction of the cell previously defined. When two or more saccade-related Purkinje cells were simultaneously isolated, the direction of the adaptation was a compromise between the preferred directions of the individual cell under recording. When the PC did not show any saccade-related activity, the direction of adaptation was randomly chosen. The onset of a saccade was identified by determining the point in time at which eye velocity exceeded 50º/s. The target was displaced either further out (outward adaptation) or back toward the fixation point (inward adaptation). The inward or outward target displacements amounted to 20%, 25%, or 30% of the original target step relative to the fixation point. The direction of adaptation was randomized from one learning session to the other. Trials containing this intrasaccadic target displacement were repeated several hundred times until a maximal and stable saccadic gain change had been achieved. Gain is defined here as the ratio of saccade amplitude and initial target amplitude. The gain change is given by the formula: gain change = [(gain before adaptation − gain during adaptation)/gain before adaptation] × 100.

Electrophysiology

Postsurgical anatomical MRI was used to facilitate the localization of lobules VI and VIIA. The identification of this part of the cerebellum was supported by the characteristically dense saccade-related granule-cell background activity and the large number of saccade-related single units. All recordings were conducted with the monkey in complete darkness. Extracellular action potentials were recorded with commercial glass-coated tungsten microelectrodes (Alpha Omega Engineering, Nazareth, Israel; impedance < 1.2 MΩ), via a 4-probe multielectrode system (Electrode Positioning System and Multi-Channel Processor, Alpha Omega Engineering). Purkinje cells were identified by the presence of spontaneous complex spike discharge [25]. Simple and complex spikes of well-isolated PC were discriminated online by a Multi Spikes Detector (MSD, Alpha Omega Engineering). The Multi Spike Detector is designed for detecting spiky waveforms and sorting them according to shape employing an algorithm originally suggested by Worgotter et al. [26]. In short, the electrode signal is compared continuously against a template, typically based on exemplary spikes chosen by the investigator, that consists of eight points that can be adjusted manually or automatically in order to account for gradual changes in spike waveform over time. When the match between the signal and the template meets the statistical criteria, detection is reported. Figure 2 depicts a typical

example of PC records, sorted into a simple (left) and a complex (right) spike category. In this example, the average simple spike firing rate was 63.7 Hz, whereas the average complex spike firing rate was 0.9 Hz. Note that spikes with sudden changes of their morphology were excluded from further consideration. We recorded isolated PC simultaneously from up to four independently movable electrodes (Electrode Positioning System, Alpha Omega Engineering). Each PC was observed during a preadaptation baseline session and during saccadic adaptation. Only PC recorded long enough for seeing a stable gain change of at least 10% were considered in the analysis.

Data Analysis: Information on "Motor Error" Conveyed by CS

In order to test whether CS conveys information on the size of the motor error, we used an information analysis approach as suggested by Kitazawa [9]. The first step was to determine the predictive information associated with the occurrence of complex spikes (I_{cs}). I_{cs} was quantified for periods of 20 ms as the decrease in entropy of the absolute motor error for this period as given by

$$I_{cs} = \sum_{i=1}^{2} -[(n_i/N)\cdot\log_2(n_i/N)] - \sum_{i=1}^{2} -[(m_i/M)\cdot\log_2(m_i/M)], \quad (1)$$

with n_i denoting the total number of trials in the i^{th} pool and m_i the number of trials with CS in the i^{th} pool; N denotes the total numbers of trials in both pools, the first one containing the 50% of trials with the smallest motor error, the second one containing the 50% of trials with the largest motor error, and M the total number of trials with CS. If trials with CS were confined to only one pool, Equation 1 would yield 1 bit for I_{cs}. Conversely, if CS were distributed evenly in the two pools, I_{cs} would be 0.

Not only the occurrence but, alternatively, also the omission of a CS could provide information on the size of the motor error. The variant of Equation 1, describing the decrease in entropy of the absolute motor error associated with the omission of CS $I_{\overline{cs}}$, is given by

$$I_{\overline{cs}} = \sum_{i=1}^{2} -[(n_i/N)\cdot\log_2(n_i/N)] - \sum_{i=1}^{2} -[((n_i-m_i)/(N-M))\cdot\log_2((n_i-m_i)/(N-M))]. \quad (2)$$

The notation is the same as in Equation 1. $(n_i - m_i)$ denotes the number of trial during which no CS were recorded in pool i^{th}, and $(N - M)$ is the total number of trials in which no CS were recorded in a given time window.

The total information (I) on the size of the motor error carried by the CS firing pattern is given by

$$I = p\cdot I_{cs} + (1-p)\cdot I_{\overline{cs}}, \quad (3)$$

where p is the probability of CS within the period of time under consideration. In order to express the amount of information per period of time, we finally calculated the "information transmission rate," I_r, as given by

$$I_r = I/W, \quad (4)$$

where W denotes the width of the time windows. As mentioned before, we used time windows of 20 ms for all neurons considered. To test whether the counts are evenly distributed or not, we used chi-square statistics. When the p value was larger than 0.05, we discarded the information and regarded it as zero.

As discussed in the main text, rather than reflecting the size of the motor error, the population averages seemed to suggest a gradual build-up of specific CS patterns during adaptation. If this impression is correct, CS should convey information on the state of adaptation as captured by trial number. Hence, we adapted the approach described in the preceding sections in order to allow us to assess whether CS conveyed information on trial number. The decisive step is to sort trials into two pools reflecting the 50% earliest and the 50% latest trials.

Acknowledgments

We are grateful to Dr. Kitazawa for his valuable advice on the application of information theory. This work was made possible by grants from the Schilling Foundation and the Deutsche Forschungsgemeinschaft (SFB 550). The authors declare no competing financial interest.

Received: September 2, 2005
Revised: October 21, 2005
Accepted: November 8, 2005
Published: December 19, 2005

References

1. Kommerell, G., Olivier, D., and Theopold, H. (1976). Adaptive programming of phasic and tonic components in saccadic eye movements. Investigations of patients with abducens palsy. Invest. Ophthalmol. *15*, 657–660.
2. McLaughlin, S.C. (1967). Parametric adjustment in saccadic eye movements. Percept. Psychophys. *2*, 359–362.
3. Hopp, J.J., and Fuchs, A.F. (2004). The characteristics and neuronal substrate of saccadic eye movement plasticity. Prog. Neurobiol. *72*, 27–53.
4. Barash, S., Melikyan, A., Sivakov, A., Zhang, M., Glickstein, M., and Thier, P. (1999). Saccadic dysmetria and adaptation after lesions of the cerebellar cortex. J. Neurosci. *19*, 10931–10939.
5. Marr, D. (1969). A theory of cerebellar cortex. J. Physiol. *202*, 437–470.
6. Albus, J.S. (1971). A theory of cerebellar function. Math. Biosci. *10*, 25–61.
7. Palkovits, M., Mezey, E., Hamori, J., and Szentagothai, J. (1977). Quantitative histological analysis of the cerebellar nuclei in the cat. I. Numerical data on cells and on synapses. Exp. Brain Res. *28*, 189–209.
8. Monsivais, P., Clark, B.A., Roth, A., and Hausser, M. (2005). Determinants of action potential propagation in cerebellar Purkinje cell axons. J. Neurosci. *25*, 464–472.
9. Kitazawa, S., Kimura, T., and Yin, P.B. (1998). Cerebellar complex spikes encode both destinations and errors in arm movements. Nature *392*, 494–497.
10. Kahlon, M., and Lisberger, S.G. (2000). Changes in the responses of Purkinje cells in the floccular complex of monkeys after motor learning in smooth pursuit eye movement. J. Neurophysiol. *84*, 2945–2960.
11. Yakushin, S.B., Reisine, H., Buttner-Ennever, J., Raphan, T., and Cohen, B. (2000). Functions of the nucleus of the optic tract (NOT). I. Adaptation of the gain of the horizontal vestibulo-ocular reflex. Exp. Brain Res. *131*, 416–432.
12. Demer, J.L., and Robinson, D.A. (1982). Effects of reversible lesions and stimulation of olivocerebellar system on vestibulooocular reflex plasticity. J. Neurophysiol. *47*, 1084–1107.
13. Ito, M. (1984). The Cerebellum and Neural Control (New York: Raven Press).
14. Sugihara, I., and Shinoda, Y. (2004). Molecular, topographic, and functional organization of the cerebellar cortex: a study with combined aldolase C and olivocerebellar labeling. J. Neurosci. *24*, 8771–8785.
15. Bergeron, A., Matsuo, S., and Guitton, D. (2003). Superior colliculus encodes distance to target, not saccade amplitude, in multi-step gaze shifts. Nat. Neurosci. *6*, 404–413.
16. Bergeron, A., and Guitton, D. (2002). In multiple-step gaze shifts: omnipause (OPNs) and collicular fixation neurons encode gaze position error; OPNs gate saccades. J. Neurophysiol. *88*, 1726–1742.
17. Krauzlis, R.J., Basso, M.A., and Wurtz, R.H. (1997). Shared motor error for multiple eye movements. Science *276*, 1693–1695.
18. Optican, L.M., and Quaia, C. (2002). Distributed model of collicular and cerebellar function during saccades. Ann. N Y Acad. Sci. *956*, 164–177.
19. Llinas, R., Baker, R., and Sotelo, C. (1974). Electrotonic coupling between neurons in cat inferior olive. J. Neurophysiol. *37*, 560–571.
20. Leznik, E., and Llinas, R. (2005). Role of gap junctions in synchronized neuronal oscillations in the inferior olive. J. Neurophysiol. *94*, 2447–2456.

21. Ito, M. (2001). Cerebellar long-term depression: characterization, signal transduction, and functional roles. Physiol. Rev. *81*, 1143–1195.
22. Wang, S.S., Denk, W., and Hausser, M. (2000). Coincidence detection in single dendritic spines mediated by calcium release. Nat. Neurosci. *3*, 1266–1273.
23. Thier, P., Dicke, P.W., Haas, R., and Barash, S. (2000). Encoding of movement time by populations of cerebellar Purkinje cells. Nature *405*, 72–76.
24. Judge, S.J., Richmond, B.J., and Chu, F.C. (1980). Implantation of magnetic search coils for measurement of eye position: an improved method. Vision Res. *20*, 535–538.
25. Thach, W.T. (1968). Discharge of Purkinje and cerebellar nuclear neurons during rapidly alternating arm movements in the monkey. J. Neurophysiol. *31*, 785–797.
26. Worgotter, F., Daunicht, W.J., and Eckmiller, R. (1986). An online spike form discriminator for extracellular recordings based on an analog correlation technique. J. Neurosci. Methods *17*, 141–151.